Low-frequency noise in AlTiO/AlGaN/GaN metal-insulator-semiconductor heterojunction field-effect transistors

Son Phuong Le, Toshimasa Ui, Tuan Quy Nguyen, Hong-An Shih, and Toshi-kazu Suzuki[a)]
Center for Nano Materials and Technology, Japan Advanced Institute of Science and Technology (JAIST), 1-1 Asahidai, Nomi, Ishikawa 923-1292, Japan

(Received 25 March 2016; accepted 10 May 2016; published online 27 May 2016)

Using aluminum titanium oxide (AlTiO, an alloy of Al_2O_3 and TiO_2) as a high-k gate insulator, we fabricated and investigated AlTiO/AlGaN/GaN metal-insulator-semiconductor heterojunction field-effect transistors. From current low-frequency noise (LFN) characterization, we find Lorentzian spectra near the threshold voltage, in addition to 1/f spectra for the well-above-threshold regime. The Lorentzian spectra are attributed to electron trapping/detrapping with two specific time constants, ~25 ms and ~3 ms, which are independent of the gate length and the gate voltage, corresponding to two trap level depths of 0.5–0.7 eV with a 0.06 eV difference in the AlTiO insulator. In addition, gate leakage currents are analyzed and attributed to the Poole-Frenkel mechanism due to traps in the AlTiO insulator, where the extracted trap level depth is consistent with the Lorentzian LFN. *Published by AIP Publishing*. [http://dx.doi.org/10.1063/1.4952386]

I. INTRODUCTION

GaN-based metal-insulator-semiconductor heterojunction field-effect transistors (MIS-HFETs) with various high-dielectric-constant (high-k) gate insulators, such as Al_2O_3,[1] HfO_2,[2,3] ZnO,[4] TaON,[5] AlN,[6–9] or BN,[10,11] have been extensively developed, owing to the merits of gate leakage reduction and passivation effects. Although both a high k and a wide energy gap (E_g) are important for a gate insulator, there exists a trade-off between these two properties.[12] One effective method to balance k and E_g is employing aluminum titanium oxide (AlTiO, an alloy of Al_2O_3 and TiO_2) with intermediate physical properties of Al_2O_3 ($k \sim 9$, $E_g \sim 7$ eV) and TiO_2 ($k \sim 60$, $E_g \sim 3$ eV). AlTiO has been used for Si-based devices[13–15] and GaAs-based devices[16,17] and also should be promising for GaN-based MIS-HFETs. On the other hand, current low-frequency noise (LFN) in MIS devices might be influenced by electron traps, in particular, by those related to gate insulators.[18] In fact, in addition to 1/f LFN spectra,[19–27] Lorentzian LFN spectra are sometimes observed,[28–31] being attributed to electron traps in GaN-based HFETs. Therefore, LFN characterization is an important diagnostic tool for electron traps in GaN-based MIS-HFETs.

In this work, we fabricated and investigated AlTiO/AlGaN/GaN MIS-HFETs using an Al_xTi_yO ($x : y = 0.73 : 0.27$) gate insulator ($k \sim 14$, $E_g \sim 6$ eV), obtained by atomic layer deposition (ALD). From current LFN characterization, we find Lorentzian spectra near the threshold voltage, attributed to electron trapping/detrapping in the AlTiO insulator, from which we extracted time constants as well as trap level depths. Moreover, gate leakage currents are analyzed and attributed to the Poole-Frenkel mechanism due to traps in the AlTiO insulator, which are discussed in relation with the Lorentzian LFN.

[a)]Author to whom correspondence should be addressed. Electronic mail: tosikazu@jaist.ac.jp

II. DEVICE FABRICATION AND BASIC CHARACTERISTICS

Using an $Al_{0.27}Ga_{0.73}N$(30 nm)/GaN(3000 nm) heterostructure obtained by metal-organic vapor phase epitaxy on sapphire(0001), we fabricated AlTiO/AlGaN/GaN MIS devices as follows. On the AlGaN/GaN heterostructure, Ti/Al/Ti/Au Ohmic electrodes were formed, and device isolation was achieved by B^+ ion implantation. After AlGaN surface treatments, a 29-nm-thick Al_xTi_yO ($x : y = 0.73 : 0.27$) film as a gate insulator was deposited by ALD using trimethyl aluminum (TMA), tetrakisdimethylamino titanium (TDMAT), and H_2O.[17] Considering the trade-off between k and E_g as well as the break-down field F_b, we employed Al_xTi_yO with $x : y = 0.73 : 0.27$, which has $k \sim 14$ (the static dielectric constant obtained by capacitance measurements of metal-insulator-metal structures at $\leq$1 MHz), $E_g \sim 6$ eV, and $F_b \sim 6.5$ MV/cm.[17] Hall-effect measurements show an electron mobility of 1450 cm^2/V-s, a sheet electron concentration of 9.1×10^{12} cm^{-2}, and a sheet resistance of 470 Ω/□ of the two-dimensional electron gas (2DEG) of the AlTiO/AlGaN/GaN. Finally, the formation of Ni/Au gate electrodes on the AlTiO followed by an annealing at 350 °C for 30 min in H_2-mixed (10%) Ar ambience completed the device fabrication. As a result, we obtained AlTiO/AlGaN/GaN MIS-HFETs, MIS capacitors, and ungated two-terminal (2T) devices as shown in Fig. 1. The MIS-HFETs have gate lengths of $L_G = 0.26$, 0.56, and 1.1 μm, a source-drain spacing of 5 μm, a source-gate spacing of 2 μm, and a channel width of $W = 50$ μm. The MIS capacitors have a gate area of 100 μm × 100 μm, distanced 25 μm apart from the Ohmic electrode. The ungated 2T devices have channel lengths (electrode spacings) of $L = 2$–16 μm and a channel width of $W = 100$ μm. It should be noted that the fabrication and characteristics (including LFN characteristics) of the baseline AlGaN/GaN Schottky-HFETs have been reported in Ref. 27.

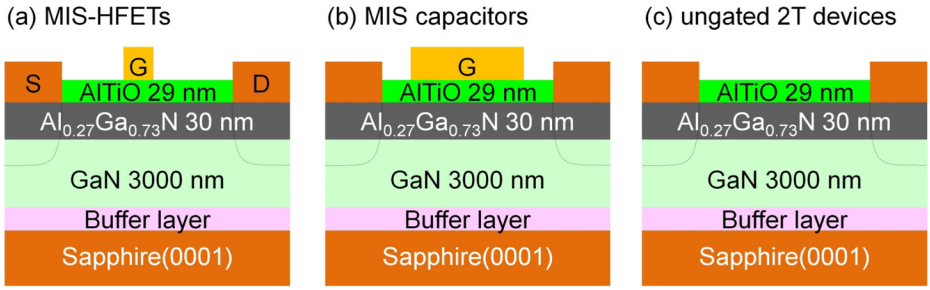

FIG. 1. Schematics of the AlTiO/AlGaN/GaN (a) MIS-HFETs, (b) MIS capacitors, and (c) ungated 2T devices.

Figure 2 shows examples of output and transfer characteristics of the AlTiO/AlGaN/GaN MIS-HFETs with $L_G = 0.26\,\mu$m, where V_D is the drain-source voltage, V_G is the gate-source voltage, I_D is the drain current, I_G is the gate current, and g_m is the transconductance. (Considering LFN characterization, we employ the definition of currents in the unit of [A] without normalization by the channel width; the vertical axis of Fig. 2 shows I_D/W and I_G/W in the unit of [mA/mm].) As shown in the output characteristics of Fig. 2(a), we obtain drain currents as high as ~700 mA/mm. The transfer characteristics at $V_D = 10$ V in the saturation regime (Fig. 2(b)) and at $V_D = 0.1$ V in the linear regime (Fig. 2(c)) both exhibit significantly small I_G of 10^{-8} A/mm range or less, about 7 and 4 orders of magnitude smaller for forward and reverse biases, respectively, than those of Schottky-HFETs, owing to good insulating properties of the AlTiO. The small gate leakage currents lead to small drain off-currents shown in Figs. 2(b) and 2(c). In addition, we observe a bump of I_G for high V_D as shown in Fig. 2(b), attributed to a self-heating effect; the bump disappears for small V_D as in Fig. 2(c). The obtained device characteristics suggest that AlTiO can be an important candidate as a gate insulator for GaN-based MIS-HFETs. We also characterized the AlTiO/AlGaN/GaN MIS capacitors. Figure 3 shows capacitance-voltage (C-V_G) characteristics at 1 MHz under $V_G = -15\,\text{V} \rightarrow +6\,\text{V}$ and the 2DEG concentration n_s under the gate calculated by the integration of C as a function of V_G. The C-V_G characteristics exhibit a quite small hysteresis less than 30 mV under $V_G = -15\,\text{V} \rightarrow +6\,\text{V}$ and $V_G = +6\,\text{V} \rightarrow -15\,\text{V}$ with a sweep rate of 0.36 V/s. From the capacitance plateau, we can estimate the dielectric constant of the AlTiO insulator, $k \sim 14$, which is consistent with the capacitance measurements of the metal-insulator-metal structures. The inset of Fig. 3 shows current density-voltage (J-V_G) characteristics of the MIS capacitors, being consistent with the gate leakage of the MIS-HFETs.

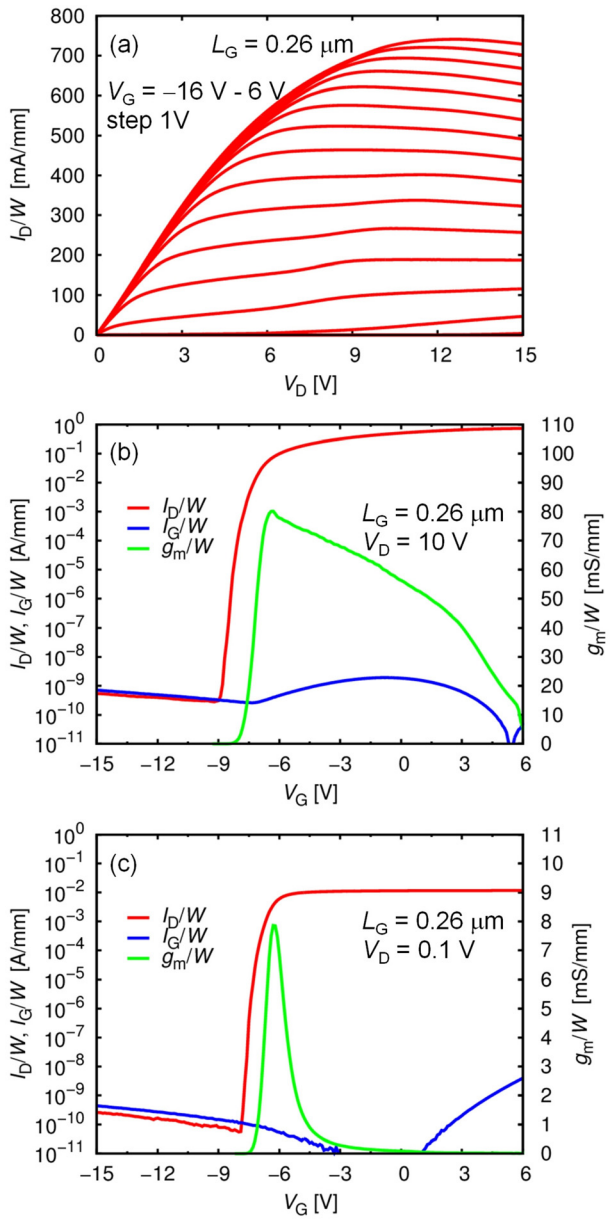

FIG. 2. (a) Output characteristics, and transfer characteristics at (b) $V_D = 10$ V and (c) $V_D = 0.1$ V of the AlTiO/AlGaN/GaN MIS-HFET with $L_G = 0.26\,\mu$m. The drain current I_D, the gate current I_G, and the transconductance g_m are normalized by the channel width W.

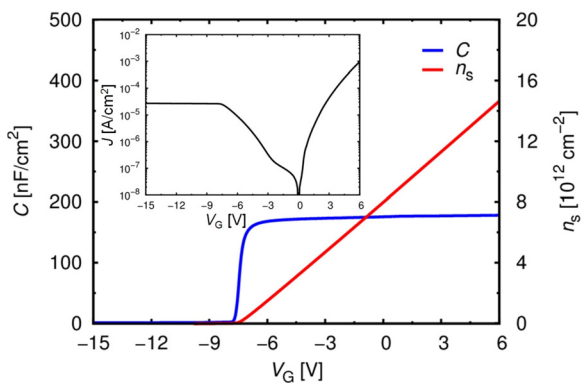

FIG. 3. C-V_G characteristics of the AlTiO/AlGaN/GaN MIS capacitor at 1 MHz and the 2DEG concentration n_s under the gate calculated by the integration of C as a function of V_G. The inset: J-V_G characteristics.

III. LOW-FREQUENCY NOISE CHARACTERISTICS

For LFN characterization of the devices, we employed a measurement system consisting of a shielded probe station, a low-noise pre-amplifier (LNA, Stanford SR570), and a dynamic signal analyzer (DSA, Agilent 35670A).[27,32] We first measured LFN in the AlTiO/AlGaN/GaN ungated 2T devices. Figure 4 shows examples of measurement results of current noise power spectrum density (PSD), S_I, as a function of the frequency f for the Ohmic regime of the ungated 2T devices with $L = 2$ and 16 μm. We observe pure $1/f$ LFN spectra satisfying $S_I/I^2 \simeq K/f$ with a constant factor K, where the DC current I is varied by changing the 2T noiseless bias voltage V. In the same way as the previous work,[27] we can identify the contributions from the Ohmic contacts and the ungated 2DEG channel by analyzing KW depending on the channel length L shown in the inset of Fig. 4. As a result, we obtain the factor K_c for one Ohmic contact and the Hooge parameter α_{ug} for the ungated 2DEG, $K_cW \simeq 1.5 \times 10^{-12}$ cm and $\alpha_{ug} \simeq 4.0 \times 10^{-4}$, which are similar to other AlGaN/GaN devices in the previous work.

We next measured LFN in the AlTiO/AlGaN/GaN MIS-HFETs. Figure 5(a) shows examples of measurement results of drain current noise PSD, S_{I_D}, for the linear regime of the AlTiO/AlGaN/GaN MIS-HFETs with $L_G = 0.26$ μm at fixed gate voltages V_G. We confirm the relation $S_{I_D} \propto {I_D}^2$, where the drain current I_D is varied by changing the noiseless drain voltage V_D. In the well-above-threshold regime, $V_G \gtrsim -4$ V, pure $1/f$ LFN spectra satisfying $S_{I_D} \simeq K_{HFET}{I_D}^2/f$ with a constant factor K_{HFET} were obtained. From the pure $1/f$ LFN spectra, we obtain Hooge parameters α in the intrinsic gated region as in the previous work.[27] Fig. 5(b) shows α for AlTiO/AlGaN/GaN MIS-HFETs as a function of the 2DEG concentration n_s under the gate given in Fig. 3, with the results for AlN/AlGaN/GaN MIS-HFETs, where the AlN gate insulator was deposited by RF magnetron sputtering,[8,9] and AlGaN/GaN Schottky-HFETs, as well as α_{ug} for the ungated 2DEG. We observe a universal behavior, which can be attributed to fluctuations in the intrinsic gate voltage through the extrinsic source resistance.[27] On the other hand, near the threshold voltage, $V_G \sim -7$–-5 V, we find non-$1/f$ LFN spectra with Lorentzian behaviors. No Lorentzian LFN spectra are observed for AlN/AlGaN/GaN MIS-HFETs and AlGaN/GaN Schottky-HFETs, which show pure $1/f$ LFN spectra for all gate biases.[27] Therefore, the Lorentzian LFN spectra are attributed to the AlTiO gate insulator.

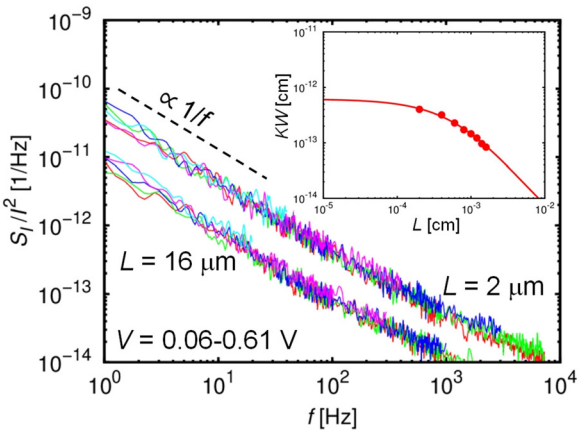

FIG. 4. LFN spectra normalized by the current square, S_I/I^2, as functions of frequency f for the AlTiO/AlGaN/GaN ungated 2T devices. The inset: KW depending on the channel length L.

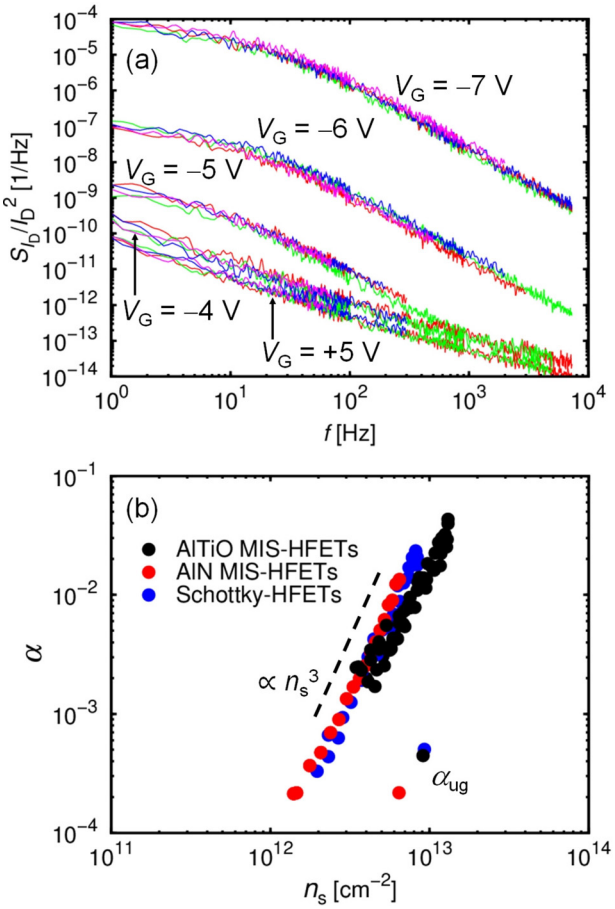

FIG. 5. (a) LFN spectra normalized by the drain current square, $S_{I_D}/{I_D}^2$, for the AlTiO/AlGaN/GaN MIS-HFETs with $L_G = 0.26$ μm. (b) Hooge parameter α as a function of n_s with the results for AlN/AlGaN/GaN MIS-HFETs and AlGaN/GaN Schottky-HFETs, as well as α_{ug} for the ungated 2DEG.

Hereafter, we discuss the Lorentzian LFN spectra. Figure 6(a) shows the observed spectra depending on the gate voltage V_G, where we can confirm that all the spectra exhibit Lorentzian behavior. The Lorentzian spectra can be well-fitted by a superposition of two Lorentzians

$$\frac{S_{I_D}(f)}{{I_D}^2} = \frac{A_1}{1+(2\pi f\tau_1)^2} + \frac{A_2}{1+(2\pi f\tau_2)^2}, \quad (1)$$

where τ_1 and τ_2 are time constants, and A_1 and A_2 are Lorentzian prefactors. Figure 6(b) shows an example of the fitting. As a result of the fitting for $L_G = 0.26$, 0.56, and 1.1 μm, we obtain time constants τ_1, τ_2, shown in Fig. 7(a), and Lorentzian prefactors A_1, A_2, as functions on the gate voltage V_G. Two specific time constants, $\tau_1 \sim 25$ ms and $\tau_2 \sim 3$ ms, are independent of V_G and L_G. The bias independent time constants suggest that the Lorentzian spectra are attributed to two electron trap levels inside the AlTiO insulator. In general, such time constant τ at temperature T is given by $\tau = 1/(v_{th}\sigma_e N_c)e^{E_a/k_BT} = \tau_0 e^{E_a/k_BT}$, where k_B is the

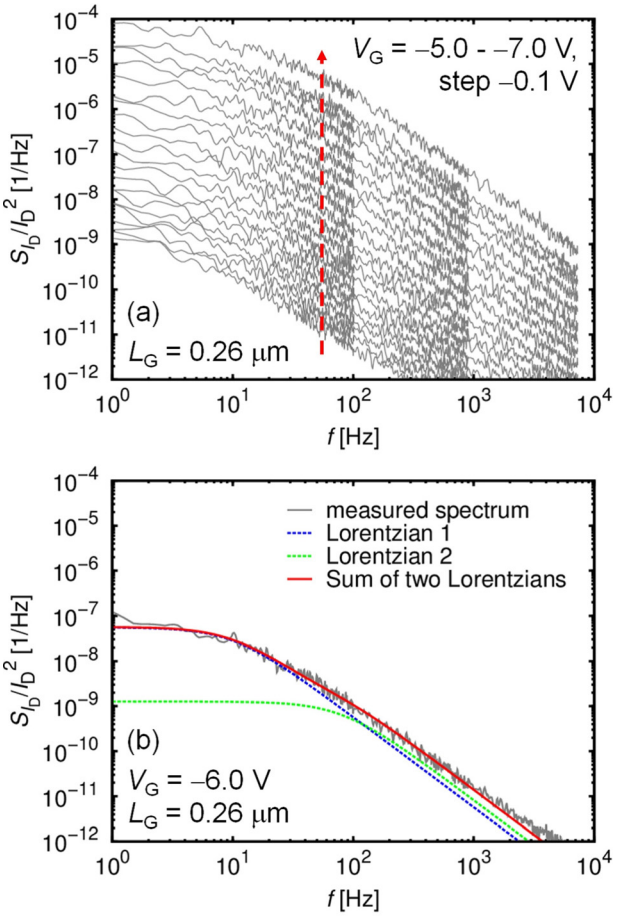

FIG. 6. (a) Lorentzian LFN spectra depending on the gate voltage V_G. (b) An example of fitting of a LFN spectrum at $V_G = -6.0$ V by a superposition of two Lorentzians.

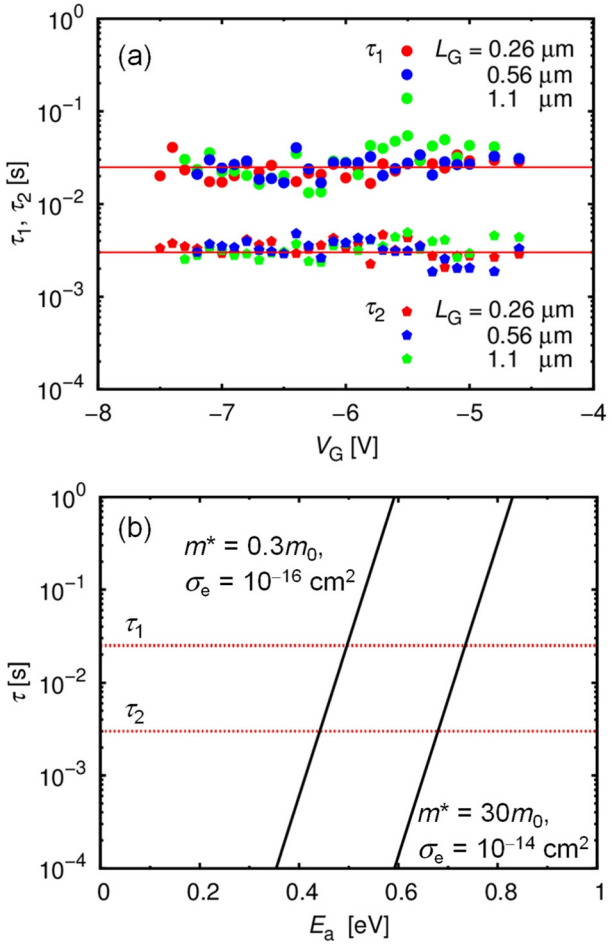

FIG. 7. (a) Time constants τ_1 and τ_2 as functions on the gate voltage V_G. (b) The relation between the time constant and the electron trap level depth E_a.

Boltzmann constant, v_{th} is the electron thermal velocity, σ_e is the electron capture cross-section, N_c is the effective density of states in the conduction band, and E_a is the trap level depth. Although we do not know the electron capture cross-section, we can estimate the trap level depths in the AlTiO insulator. As shown in Fig. 7(b), even if we assume a wide range of $\sigma_e = 10^{-16}$–10^{-14} cm^2 and an electron effective mass between $m^* = 0.3m_0$ for Al_2O_3[33] and $m^* = 30m_0$ for TiO_2[34,35] (m_0: the bare electron mass), the trap level depths are estimated to be $E_{a1} = (1/\beta)\ln(\tau_1/\tau_0) \simeq 0.5$–$0.7$ eV and $E_{a2} = E_{a1} - \Delta E_a$ with $\Delta E_a \simeq 0.06$ eV. On the other hand, the Lorentzian prefactors depend on V_G. Normalized Lorentzian prefactors, products of the prefactor and the gate area, $A_1 L_G W$ and $A_2 L_G W$, are shown in Fig. 8, as functions of (a) the gate voltages V_G and (b) the 2DEG concentration n_s under the gate. We find that $A_1 L_G W$ and $A_2 L_G W$ are independent of the gate area, i.e., the Lorentzian prefactors are inversely proportional to the gate area as a natural consequence of the law of large numbers. We observe decreases in the normalized Lorentzian prefactors with an increase in V_G as well as n_s, implying that the effects of electron trapping/detrapping are more dominant for lower 2DEG concentrations n_s. This suggests that Lorentzian LFN near the threshold voltage can be a good indicator of the quality of gate insulators. On the other hand, for the well-above-threshold regime, i.e., for large n_s, Lorentzian LFN is buried in $1/f$ spectra.

In order to understand the meaning of the Lorentzian prefactors, we consider a general Lorentzian current PSD normalized by the current square

$$\frac{S_I}{I^2} = \frac{A}{1 + (2\pi\tau f)^2} = \frac{2\pi\tau\alpha_L}{N}\frac{1}{1 + (2\pi\tau f)^2}, \tag{2}$$

with a prefactor A (in the unit of [1/Hz]) and a specific time constant τ (or a specific frequency $f_0 = 1/2\pi\tau$), where we define a dimensionless Hooge-like parameter α_L for Lorentzian LFN by $A = \alpha_L/Nf_0 = 2\pi\tau\alpha_L/N$ using the total carrier number N. Since the current fluctuation δI is given by

$$\frac{(\delta I)^2}{I^2} = \int_0^\infty \frac{S_I}{I^2} df = \frac{\pi}{2}\frac{\alpha_L}{N}, \tag{3}$$

and Burgess theorem[36] gives

$$\frac{(\delta I)^2}{I^2} = \frac{1}{N}\left[\frac{(\delta\mu)^2}{\mu^2} + \frac{(\delta N)^2}{N}\right], \tag{4}$$

where $\delta\mu$ and δN are the fluctuations of the mobility μ and the carrier number N, respectively, we obtain

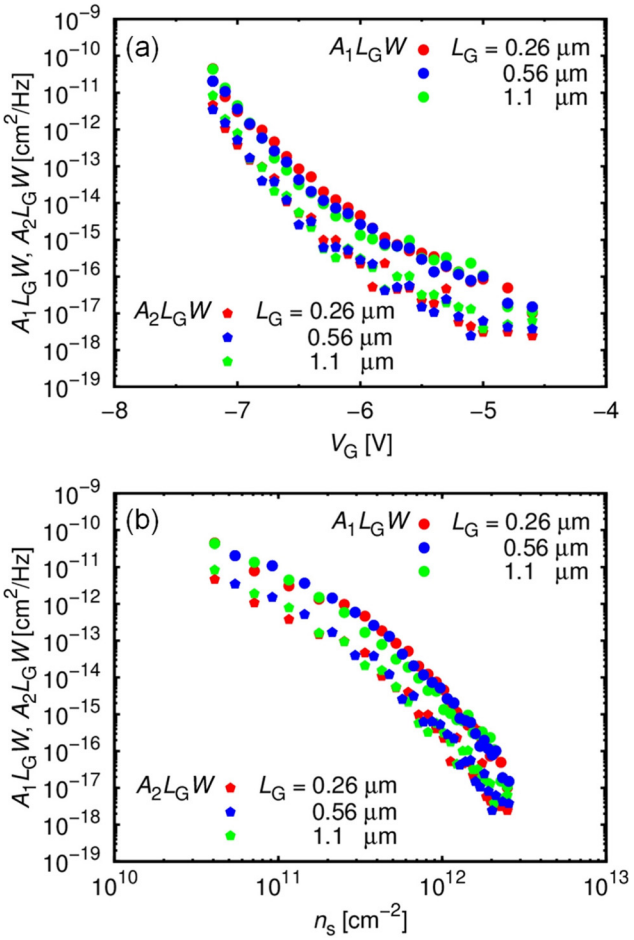

FIG. 8. Normalized Lorentzian prefactors, products of the prefactor and the gate area, A_1L_GW and A_2L_GW, as functions of (a) V_G and (b) n_s.

$$\alpha_L = \frac{2}{\pi}\left[\frac{(\delta\mu)^2}{\mu^2} + \frac{(\delta N)^2}{N}\right], \tag{5}$$

showing that the Hooge-like parameter is related to fluctuations of the mobility and carrier number. According to the definition, we evaluate Hooge-like parameters for the two Lorentzian components of the LFN in the AlTiO/AlGaN/GaN MIS-HFETs, $\alpha_{Li} = A_iN/(2\pi\tau_i)$ $(i = 1, 2)$. Figure 9 shows α_{L1} and α_{L2} as functions of n_s for $L_G = 0.26$, 0.56, and 1.1 μm, where we find $\alpha_{L1} \simeq \alpha_{L2}$. This suggests the same origin of the two trap levels in the AlTiO gate insulator. We tentatively assume an on-site Coulomb effect.[37] Although two electrons (with opposite spins) can occupy one trap level, the on-site Coulomb repulsion shifts the effective level for the second electron shallower; this gives $\Delta E_a \simeq 0.06$ eV.

IV. TRAP LEVEL DEPTH IN COMPARISON WITH AN ESTIMATION BY POOLE-FRENKEL CURRENTS

In order to confirm the AlTiO trap level depth obtained by the LFN, we investigated gate leakage currents of the MIS capacitors. Figure 10 shows the gate leakage current density J as a function of $V_R = -V_G$ at $T = 280$–380 K, dominated by the Poole-Frenkel conduction mechanism as shown below. It should be noted that we focus on reverse biases in order to accurately evaluate the electric field F in the AlTiO

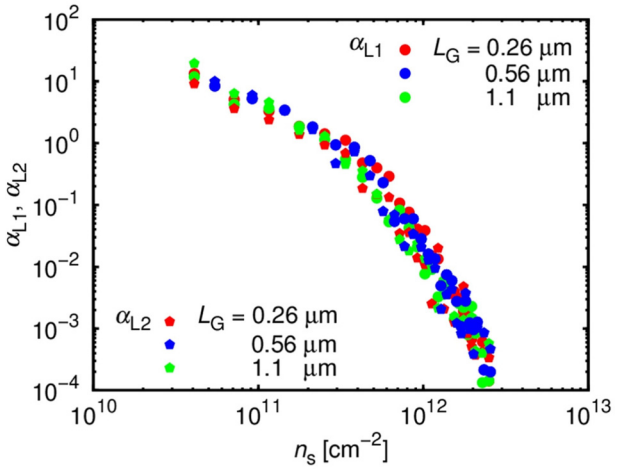

FIG. 9. The Hooge-like parameters α_{L1} and α_{L2} as functions of n_s.

gate insulator; for forward biases, it is difficult to obtain accurate F owing to effects of the interface states.[38] The electric field can be evaluated by

$$F = \frac{\Delta\sigma - qn_s}{k\varepsilon_0}, \tag{6}$$

similar to Refs. 39 and 40, where q is the electron charge, ε_0 is the vacuum permittivity, and $\Delta\sigma = \sigma - \sigma_0$ is the difference between the interface fixed charge σ at AlTiO/AlGaN and the polarization charge σ_0 of GaN. We find $\Delta\sigma/q = 7.6 \times 10^{12}\,\mathrm{cm}^{-2}$ from measurements of the MIS capacitors with several insulator thicknesses,[41,42] giving the relation between J and F shown in Fig. 11(a); Poole-Frenkel plots $(J/F - \sqrt{F})$ exhibit linear dependence in the high field regime, indicating the Poole-Frenkel conduction mechanism given by $J = BF\exp(-\beta\phi)\exp(\beta\sqrt{q^3F/(\pi\kappa\varepsilon_0)})$, where $\beta = 1/k_BT$, B is a constant, κ is related to the dielectric constant, and ϕ is the trap level depth in the AlTiO. Although we obtain $\kappa \sim 15$ from the Poole-Frenkel currents, its meaning is not clear. There exists a controversy on the meaning of the value;[43] we consider that κ can be either the static one[44] or four times of the dynamic (optical) one.[45] On the other hand, we can unambiguously obtain a trap level depth in the

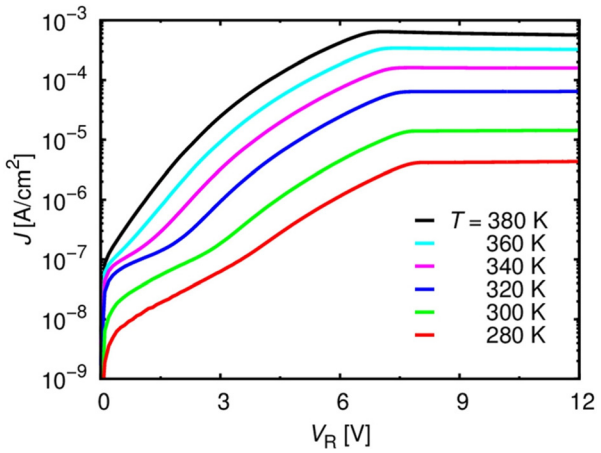

FIG. 10. Gate leakage current density J as a function of $V_R = -V_G$ at $T = 280$–380 K for the MIS capacitor.

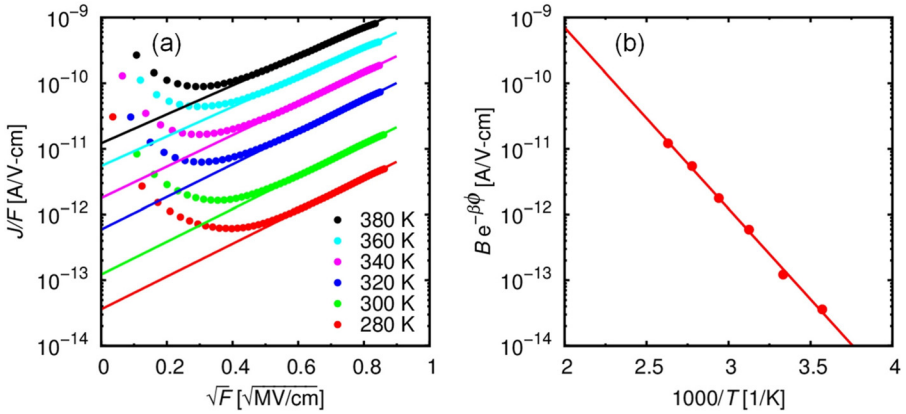

FIG. 11. (a) Poole-Frenkel plots $(J/F\text{-}\sqrt{F})$. (b) $B\exp(-\beta\phi)$ as a function of $1/T$.

AlTiO insulator $\phi \simeq 0.6$ eV by plotting $B\exp(-\beta\phi)$ as a function of $1/T$ shown in Fig. 11(b); ϕ is consistent with the trap level depth obtained from the Lorentzian LFN, indicating that the traps in the AlTiO insulator dominate both the Lorentzian LFN and the Poole-Frenkel leakage currents.

V. CONCLUSION

We fabricated and investigated AlTiO/AlGaN/GaN MIS-HFETs. From LFN characterization, in addition to $1/f$ spectra for the well-above-threshold regime, we find Lorentzian spectra near the threshold voltage, with two specific time constants ~25 ms and ~3 ms, corresponding to trap level depths of 0.5–0.7 eV. In addition, gate leakage currents are analyzed and attributed to the Poole-Frenkel mechanism due to traps in the AlTiO insulator, where the extracted trap level depth is consistent with the Lorentzian LFN, indicating that the traps in the AlTiO insulator dominate both the Lorentzian LFN and the Poole-Frenkel leakage currents. The results exemplify the importance of LFN characterization for GaN-based MIS-HFETs as a diagnostic tool.

ACKNOWLEDGMENTS

This work was supported by JSPS KAKENHI Grant Nos. 26249046 and 15 K13348.

[1]T. Hashizume, S. Ootomo, and H. Hasegawa, Appl. Phys. Lett. **83**, 2952 (2003).
[2]C. Liu, E. F. Chor, and L. S. Tan, Appl. Phys. Lett. **88**, 173504 (2006).
[3]A. Kawano, S. Kishimoto, Y. Ohno, K. Maezawa, T. Mizutani, H. Ueno, T. Ueda, and T. Tanaka, Phys. Status Solidi C **4**, 2700 (2007).
[4]Y.-L. Chiou, C.-S. Lee, and C.-T. Lee, Appl. Phys. Lett. **97**, 032107 (2010).
[5]T. Sato, J. Okayasu, M. Takikawa, and T. Suzuki, IEEE Electron Device Lett. **34**, 375 (2013).
[6]Y. Liu, J. A. Bardwell, S. P. McAlister, S. Rolfe, H. Tang, and J. B. Webb, Phys. Status Solidi C **0**, 69 (2002).
[7]R. Stoklas, D. Gregušová, Š. Gaži, J. Novák, and P. Kordoš, J. Vac. Sci. Technol., B **29**, 01A809 (2011).
[8]H.-A. Shih, M. Kudo, M. Akabori, and T. Suzuki, Jpn. J. Appl. Phys., Part 1 **51**, 02BF01 (2012).
[9]H.-A. Shih, M. Kudo, and T. Suzuki, Appl. Phys. Lett. **101**, 043501 (2012).
[10]J.-C. Gerbedoen, A. Soltani, M. Mattalah, M. Moreau, P. Thevenin, and J.-C. D. Jaeger, Diamond Relat. Mater. **18**, 1039 (2009).
[11]T. Q. Nguyen, H.-A. Shih, M. Kudo, and T. Suzuki, Phys. Status Solidi C **10**, 1401 (2013).
[12]J. Robertson, Rep. Prog. Phys. **69**, 327 (2006).
[13]O. Auciello, W. Fan, B. Kabius, S. Saha, J. A. Carlisle, R. P. H. Chang, C. Lopez, E. A. Irene, and R. A. Baragiola, Appl. Phys. Lett. **86**, 042904 (2005).
[14]L. Shi, Y. D. Xia, B. Xu, J. Yin, and Z. G. Liu, J. Appl. Phys. **101**, 034102 (2007).
[15]I. Jogi, K. Kukli, M. Kemell, M. Ritala, and M. Leskela, J. Appl. Phys. **102**, 114114 (2007).
[16]C. Mahata, S. Mallik, T. Das, C. K. Maiti, G. K. Dalapati, C. C. Tan, C. K. Chia, H. Gao, M. K. Kumar, S. Y. Chiam, H. R. Tan, H. L. Seng, D. Z. Chi, and E. Miranda, Appl. Phys. Lett. **100**, 062905 (2012).
[17]T. Ui, M. Kudo, and T. Suzuki, Phys. Status Solidi C **10**, 1417 (2013).
[18]L. Vandamme, IEEE Trans. Electron Devices **41**, 2176 (1994).
[19]M. E. Levinshtein, F. Pascal, S. Contreras, W. Knap, S. L. Rumyantsev, R. Gaska, J. W. Yang, and M. Shur, Appl. Phys. Lett. **72**, 3053 (1998).
[20]J. A. Garrido, B. E. Foutz, J. A. Smart, J. R. Shealy, M. J. Murphy, W. J. Schaff, L. F. Eastman, and E. Muñoz, Appl. Phys. Lett. **76**, 3442 (2000).
[21]S. L. Rumyantsev, N. Pala, M. S. Shur, M. E. Levinshtein, M. Asif Khan, G. Simin, and J. Yang, J. Appl. Phys. **93**, 10030 (2003).
[22]H.-C. Chiu, C.-H. Chen, H.-L. Kao, F.-T. Chien, P.-K. Weng, Y.-T. Gau, and H.-W. Chuang, Microelectron. Reliab. **53**, 1897 (2013).
[23]N. Pala, R. Gaska, S. Rumyantsev, M. Shur, M. A. Khan, X. Hu, G. Simin, and J. Yang, Electron. Lett. **36**, 268 (2000).
[24]S. L. Rumyantsev, N. Pala, M. S. Shur, R. Gaska, M. E. Levinshtein, M. A. Khan, G. Simin, X. Hu, and J. Yang, J. Appl. Phys. **88**, 6726 (2000).
[25]Y.-Z. Chiou, Y.-K. Su, J. Gong, S.-J. Chang, and C.-K. Wang, Jpn. J. Appl. Phys., Part A **45**, 3405 (2006).
[26]L.-H. Huang, S.-H. Yeh, and C.-T. Lee, Appl. Phys. Lett. **93**, 043511 (2008).
[27]S. P. Le, T. Q. Nguyen, H.-A. Shih, M. Kudo, and T. Suzuki, J. Appl. Phys. **116**, 054510 (2014).
[28]A. Balandin, S. Morozov, G. Wijeratne, S. J. Cai, R. Li, J. Li, K. L. Wang, C. R. Viswanathan, and Y. Dubrovskii, Appl. Phys. Lett. **75**, 2064 (1999).
[29]C. Kayis, J. H. Leach, C. Y. Zhu, M. Wu, X. Li, Ü. Özgür, H. Morkoç, X. Yang, V. Misra, and P. Handel, IEEE Electron Device Lett. **31**, 1041 (2010).
[30]C. Kayis, J. H. Leach, C. Y. Zhu, M. Wu, X. Li, Ü. Özgür, H. Morkoç, X. Yang, V. Misra, and P. H. Handel, Phys. Status Solidi C **8**, 1539 (2011).
[31]C. Kayis, C. Y. Zhu, M. Wu, X. Li, Ü. Özgür, and H. Morkoç, J. Appl. Phys. **109**, 084522 (2011).
[32]S. P. Le, T. Ui, and T. Suzuki, Appl. Phys. Lett. **107**, 192103 (2015).
[33]M. L. Huang, Y. C. Chang, C. H. Chang, T. D. Lin, J. Kwo, T. B. Wu, and M. Hong, Appl. Phys. Lett. **89**, 012903 (2006).
[34]B. Enright and D. Fitzmaurice, J. Phys. Chem. **100**, 1027 (1996).
[35]M. D. Stamate, Appl. Surf. Sci. **205**, 353 (2003).
[36]R. E. Burgess, J. Phys. Chem. Solids **22**, 371 (1961).
[37]M. Grundmann, *The Physics of Semiconductors* (Springer, 2010), p. 216.
[38]H.-A. Shih, M. Kudo, and T. Suzuki, J. Appl. Phys. **116**, 184507 (2014).
[39]D. Yan, H. Lu, D. Cao, D. Chen, R. Zhang, and Y. Zheng, Appl. Phys. Lett. **97**, 153503 (2010).
[40]S. Ganguly, A. Konar, Z. Hu, H. Xing, and D. Jena, Appl. Phys. Lett. **101**, 253519 (2012).
[41]S. Ganguly, J. Verma, G. Li, T. Zimmermann, H. Xing, and D. Jena, Appl. Phys. Lett. **99**, 193504 (2011).
[42]M. Ťapajna, M. Jurkovič, L. Valik, Š. Haščík, D. Gregušová, F. Brunner, E.-M. Cho, T. Hashizume, and J. Kuzmík, J. Appl. Phys. **116**, 104501 (2014).
[43]D. S. Jeong, H. B. Park, and C. S. Hwang, Appl. Phys. Lett. **86**, 072903 (2005).
[44]N. F. Mott, Philos. Mag. **24**, 911 (1971).
[45]J. G. Simmons, Phys. Rev. **155**, 657 (1967).